

Effect of thulium boro-tellurite glass system on radiation shielding parameters

A. Azuraida^{a,*}, O. Nurshahidah^a, W. Y. W. Yusoff^a, R. Falihan^a,
N. A. Abdul-Manaf^a, N. Ahmad^a

^a*Physics Department, Centre for Defence Foundation Studies, Universiti
Pertahanan Nasional Malaysia, 57000 Sungai Besi, Kuala Lumpur, Malaysia.*

This article reports the influence of thulium oxide on gamma shielding parameters of $(\text{B}_2\text{O}_3)_{0.2-x}(\text{TeO}_2)_{0.5}(\text{Bi}_2\text{O}_3)_{0.3}(\text{Tm}_2\text{O}_3)_x$ glass system. The mass attenuation coefficient has been obtained by the WinXCom program, whereas the effective atomic number and the electron density have been calculated from a comprehensive and consistent set of formulas. Appreciable variations have been observed for all parameters by varying the chemical composition of the glass and the gamma photon energy. The theoretical results have shown that the addition of the rare-earth oxide, Tm_2O_3 into the glass system as the dopant attenuates more gamma irradiation and improves the radiation shielding properties of the glass system. The interactions between the photons and the glass materials have been explained by the Photoelectric Effect, Compton Scattering and Pair Production.

(Received November 18, 2021; Accepted March 8, 2022)

Keywords: Thulium, Boro-tellurite, Mass attenuation coefficient

1. Introduction

The rising use of high-energy ionizing radiations, particularly gamma rays in many scientific and technological fields causes radioactive pollution which poses a number of radiation hazards to humans and the environment, necessitating the development of radiation safety and protection to limit the radiation to safe and acceptable levels and to minimize the radiation exposure effects. Excessive radiation exposure can cause radiation sickness and also result in long-term health effects such as cancer and cardiovascular disease. Therefore, safeguarding the human population and the environment from the harmful effects of radiation is critical and as radiation applications continue to be viable in many human activities, effective shielding against nuclear radiation is always in need for a secure living and a healthy environment.

In the field of gamma radiation shielding, it is important to understand the radiation interaction with matter, the absorption and attenuation of gamma energy in materials and to study the parameters of the shielding effectiveness of materials such as the mass attenuation coefficient (μ_m), mean free path (mfp), half value layer (HVL), effective atomic number (Z_{eff}), electron number (N_e) and exposure buildup factor (EBF) in order to develop appropriate shielding materials. Although the type of material used depends on the application, good radiation protection candidates are materials with excellent optical transparency and great radiation attenuation properties such as optical glasses. A good shielding glass combine high shielding capability and resistance against ionizing irradiation and ensures full protection for those who work in potentially dangerous areas, such as nuclear power plants or hospital x-ray rooms.

For gamma shielding, the glasses must possess high density, large atomic number, high absorption cross-section, and light elements in composition (e.g., B, Li) for an efficient elastic scattering. In this regard, heavy metal oxides such as bismuth oxide (Bi_2O_3) (density = 8.9 g/cm³) based glass is highly desirable due to its large effective atomic number (Z_{eff}), high density, and non-toxicity making it an excellent substitute for lead. In shielding glass applications, the glasses' compositions are the most important factor and the weight fraction of the glass system determines the attenuation effect. The greater the weight fraction of the high atomic number and density elements in the compositions, the more photons are attenuated [1].

* Corresponding author: azuraida@upnm.edu.my
<https://doi.org/10.15251/JOR.2022.182.141>

Earlier works reported that adding bismuth as a chemical modifier to boro-tellurite (B_2O_3 - TeO_2) glasses increases the glass density, improves the structural and optical properties and also demonstrate good shielding properties [1-4]. Boro-tellurite glasses have been extensively studied due to the unique physical properties of tellurites and their industrial importance in the production of glasses with desirable structural and optical properties.

The properties of boro-tellurite glasses doped with noble metal or rare earth elements have also been extensively studied due to their unique optical properties that make them appropriate for important applications in optics, electronics and telecommunications [5-6]. Also several works reported improved shielding performance for these glasses [7-9]. Among all rare earth ions, thulium is particularly intriguing as it can have important spectroscopic characteristics such as a fluorescence that is highly sensitive to the local environment of the Tm^{3+} ions [10], a persistent spectral hole burning that can be carried out at room temperature making it a viable option for high-density optical data storage [11].

The aim of this work is to determine theoretically the shielding parameters such as the mass attenuation coefficient (μ_m), effective atomic number (Z_{eff}), and electron density (N_{el}) of Bismuth- Boro-Tellurite doped thulium oxide glass system $[(B_2O_3)_{0.2-x}(TeO_2)_{0.5}(Bi_2O_3)_{0.3}(Tm_2O_3)_x]$ using WinXCom program in the energy range of 1keV-100GeV. Early works reported the mass attenuation coefficients for various glass systems obtained by WinXCOM demonstrated excellent accuracy comparable to the experimental results [12-15]. The theoretical calculation of the shielding parameters also applies to polymers [16], concretes [17], alloys [18] and compounds [19-21]. The theoretical results by WinXcom [19-21] were found to be in agreement with the experimental values.

In this study, boro-tellurite is selected as the base glass due to its specific and desirable characteristics, such as high transparency and good gamma shielding properties when combined with heavy metal oxides. The addition of bismuth oxide (Bi_2O_3) as the glass modifier is expected to improve the shielding properties. As an innovative trial, the high density rare earth element, thulium oxide (Tm_2O_3) is added to the glass system as the dopant to replace lead.

2. Theoretical calculation for shielding parameter

Based on the mixture rule shown below, the theoretical values of the mass attenuation coefficients of a mixture or compound are determined by WinXCom program [22].

$$\mu_m = \sum_i w_i (\mu_m)_i \quad (1)$$

where w_i is the weight fraction of element and $(\mu_m)_i$ is the mass attenuation coefficient for individual element. The total atomic cross-section ($\sigma_{t,a}$) can be determined from the value of the mass attenuation coefficients obtained using the following relation [23].

$$\sigma_{t,a} = \frac{\mu_m}{N_A \sum_i (w_i/A_i)} \quad (2)$$

where N_A is Avogadro's number and A_i is atomic weight of constituent element. The total electronic cross-section ($\sigma_{t,el}$) for the element is expressed by the following formula [23]:

$$\sigma_{t,el} = \frac{1}{N_A} \sum_i^n \frac{f_i A_i}{Z_i} (\mu_m)_i \quad (3)$$

where f_i is the number of atoms of element i relative to the total number of atoms of all elements in the glass material and Z_i is the atomic number of the i th element. The total atomic cross-section and the total electronic cross-section are related to the effective atomic number (Z_{eff}) of the compound by the following relation [23]:

$$Z_{eff} = \frac{\sigma_{t,a}}{\sigma_{t,el}} \quad (4)$$

The electron density can be defined as the number of electrons per unit mass, and it can be mathematically written as follows [24]:

$$N_{el} = \frac{\mu_m}{\sigma_{t,el}} \quad (5)$$

3. Results and Discussion

The theoretical values of the mass attenuation coefficient, μ_m , the effective atomic number, Z_{eff} and the electron density, N_{el} of $(B_2O_3)_{0.2-x} (TeO_2)_{0.5} (Bi_2O_3)_{0.3} (Tm_2O_3)_x$ glass system are obtained in the energy range of 1keV-100GeV for different dopant (Tm_2O_3) concentration. Table 1 shows the chemical composition for each glass sample with different concentration of Tm_2O_3 . Fig. 1 shows the variation of the theoretical values of the μ_m for each glass sample in the energy range of 1keV-100GeV. The μ_m values at photon energy of 662 keV are also obtained and recorded in Table 2.

Table 1. Chemical composition of $(B_2O_3)_{0.2-x} (TeO_2)_{0.5} (Bi_2O_3)_{0.3} (Tm_2O_3)_x$ glass system for different dopant (Tm_2O_3) concentration (mole fraction).

Glass Code (%)	Mole fraction of Tm_2O_3 (x)	Chemical composition
BiBTe	0	$(B_2O_3)_{0.2} (TeO_2)_{0.5} (Bi_2O_3)_{0.3}$
0.5TmBiBTe	0.005	$(B_2O_3)_{0.195} (TeO_2)_{0.5} (Bi_2O_3)_{0.3} (Tm_2O_3)_{0.005}$
1.0TmBiBTe	0.010	$(B_2O_3)_{0.190} (TeO_2)_{0.5} (Bi_2O_3)_{0.3} (Tm_2O_3)_{0.010}$
1.5TmBiBTe	0.015	$(B_2O_3)_{0.185} (TeO_2)_{0.5} (Bi_2O_3)_{0.3} (Tm_2O_3)_{0.015}$
2.0TmBiBTe	0.020	$(B_2O_3)_{0.180} (TeO_2)_{0.5} (Bi_2O_3)_{0.3} (Tm_2O_3)_{0.020}$
2.5TmBiBTe	0.025	$(B_2O_3)_{0.175} (TeO_2)_{0.5} (Bi_2O_3)_{0.3} (Tm_2O_3)_{0.025}$
3.0TmBiBTe	0.030	$(B_2O_3)_{0.170} (TeO_2)_{0.5} (Bi_2O_3)_{0.3} (Tm_2O_3)_{0.030}$

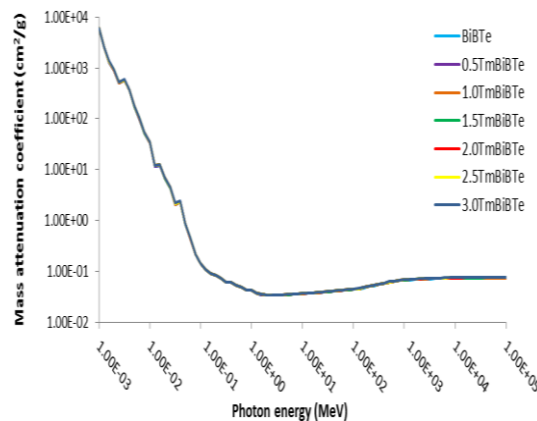


Fig. 1. Variation of the theoretical values of the mass attenuation coefficient, μ_m of $(B_2O_3)_{0.2-x} (TeO_2)_{0.5} (Bi_2O_3)_{0.3} (Tm_2O_3)_x$ glass system with different Tm_2O_3 concentration in the energy range of 1keV-100GeV.

Table 2. The theoretical values of the mass attenuation coefficient, μ_m of $(B_2O_3)_{0.2-x}(TeO_2)_{0.5}(Bi_2O_3)_{0.3}(Tm_2O_3)_x$ glass system with different Tm_2O_3 concentration at photon energy of 662 keV.

Glass code	Mass attenuation coefficient (g/cm^3)
BiBTe	0.08529
0.5TmBiBTe	0.08536
1.0TmBiBTe	0.08544
1.5TmBiBTe	0.08551
2.0TmBiBTe	0.08558
2.5TmBiBTe	0.08566
3.0TmBiBTe	0.08573

From the graph, in general, the μ_m values increase as the dopant (Tm_2O_3) concentration increases. The glass sample 3.0TmBiBT (with composition 0.03 mol of Tm_2O_3) displays the highest μ_m in the energy range of 1keV-100GeV. As can be seen clearly in Table 2, glass sample 0.170(B_2O_3) 0.5(TeO_2) 0.3(Bi_2O_3) 0.030(Tm_2O_3) gives the highest value of μ_m with 0.08573 g/cm^3 . A previous work using WinXcom studied the mass attenuation coefficients (μ/ρ) of different concentrations (0.1–2.0 mol%) of Tm^{3+} doped multicomponent borosilicate glasses with 10 mol% Li_2O or MgO within the 0.015–10 MeV energy range. The results revealed that the (μ/ρ) values for the glasses increase with the addition of Tm_2O_3 . The 2.0 mol% Tm_2O_3 doped glasses showed a better ability to attenuate gamma-rays in comparison to other glass samples, so the addition of Tm_2O_3 content leads to improvement of the shielding efficiency of the prepared glasses [25].

The decrement and increment of one μ_m line with the other μ_m lines in the graph are influenced by the photon energy, the glass density [26] and also the chemical composition of the glass. Given in Table 3 are the density values of the materials used in the glass system.

Table 3. Density values of the materials used in the glass system.

Materials	Density (g/cm^3)
Tellurium (IV) dioxide, TeO_2	5.8
Boron oxide, B_2O_3	2.46
Bismuth oxide, Bi_2O_3	8.9
Thulium (III) oxide, Tm_2O_3	8.6

For energy less than 1 MeV, the μ_m values for all glasses decrease rapidly as the photon energy increases. This is due to the Photoelectric Effect between the atoms in the glass and the gamma ray photons. In this energy region, sharp discontinuities (zigzag curve) also known as “absorption edge” can be observed from the graph. The absorption edge corresponds to the binding energy of electrons from atoms’ bound shells. A photon having an energy just above the binding energy of the electron has a tendency to be absorbed more than a photon with an energy slightly below this edge. For photons below the edge, the interaction with electrons from the shell (K, L, M and/or N) is energetically impossible and therefore the probability drops abruptly. At energy range of 1 MeV to 7 MeV ($1 \text{ MeV} < E < 7 \text{ MeV}$), the μ_m values of all glasses decrease slowly with the increment of the energy and it becomes nearly zero when the energy is almost 7 MeV. When the energy of the photon passes the maximum energy of the photoelectric interaction, the Compton Scattering mechanism takes place. Part of the total photon energy will be transferred to the electrons in the outer shells (recoil electrons) and the rest of the energy continues to scatter in

different directions at low photon energy (scattered photons). The Compton Scattering mechanism is conversely relative to the photon energy and it changes linearly with the atomic number, Z [27]. The atomic number, Z for boron, oxygen, tellurium, thulium and bismuth are 5, 8, 52, 69 and 83, respectively. At high energy region ($E > 7$ MeV), the μ_m values for all glasses increase slowly until the energy reaches 30 GeV ($E = 30$ GeV) and then become constant until the energy reaches 100 GeV ($E = 100$ GeV). In this region, the Pair Production becomes the dominant mechanism between photons and atoms inside the glass materials. Similar pattern of graphs are also shown for glass system with different composition such as in $[(\text{TeO}_2)_{0.7} (\text{B}_2\text{O}_3)_{0.3}]_{1-x} (\text{Bi}_2\text{O}_3)_x$ glass system [2]. Although glasses with Bi_2O_3 composition have higher density than BaO glasses, the graphs of their mass attenuation coefficients against photon energy display similar patterns. This shows that the variation of μ_m in the energy range of $1\text{keV} < E < 100\text{GeV}$ is not influenced by the atomic number, Z but is mainly influenced by gamma energy [2]. This behavior was also observed in the previous works by [28, 29, 30].

The values of Z_{eff} are also plotted against energy for each glass system as shown in Fig. 2. The graphs vary with gamma ray energies ranging from 1 keV to 100 GeV and the Z_{eff} values range between 16.73 and 39.42. As can be seen from the graph, the Z_{eff} values increase in the energy region of $E < 10$ KeV and decrease as the energy rises to 1 MeV. The Z_{eff} graph for all glass systems changes drastically in this energy region ($E < 1$ MeV). The drastic changes (up and down) are due to the absorption edges of Bi (K-, L- and M-edge), Te (K-, L- and M-edge) and Tm (K-, L- and M-edge). However, the low absorption edge (K-, L- and M edge) displayed for BiBTe glass, is due to only Bi and Te elements. It is well known that chemical effects are appreciable only near the absorption edges [31]. As the energy increases to 18 MeV, the Z_{eff} values show a slow increment. The Compton Scattering mechanism is dominant and the interaction cross section is directly proportional to the atomic number, Z [29]. The Z_{eff} values then become constant for energy above 100 MeV. This behavior is attributed to the dominance of Pair Production.

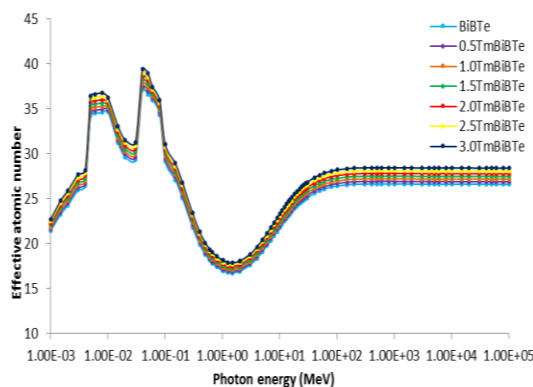


Fig. 2. Effective atomic number, Z_{eff} of $(\text{B}_2\text{O}_3)_{0.2-x} (\text{TeO}_2)_{0.5} (\text{Bi}_2\text{O}_3)_{0.3} (\text{Tm}_2\text{O}_3)_x$ glass system for different Tm_2O_3 concentration in the energy range of 1keV-100GeV.

Fig. 3. shows the variation of N_{el} against energy for each glass system. Since the graph pattern is similar to that of the Z_{eff} , a similar approach can be described. At the low energy range of $E < 0.01$ MeV, both Z_{eff} and N_{el} display the same graph pattern and both obtain maximum value due to photoelectric absorption. Over the intermediate region (0.05 MeV $< E < 5$ MeV) where Compton Scattering prevails, the two parameters decrease with energy and then become constant in the high energy region and around 100 MeV. This is attributed to the dominance of Pair Production. Similar pattern graphs of Z_{eff} and N_e for photon energies from 1keV to 100 GeV were also observed by [2, 32,33,34,35]. The Z_{eff} and N_e values were believed to be influenced by the chemical composition, molecular and thermal environment [36].

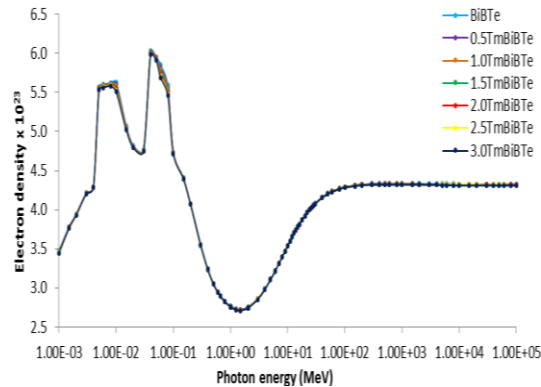


Fig. 3. Electron density, N_{el} of $(B_2O_3)_{0.2-x}(TeO_2)_{0.5}(Bi_2O_3)_{0.3}(Tm_2O_3)_x$ glass system for different Tm_2O_3 concentration in the energy range of 1keV-100GeV.

Several previous works highlighted the significance of the rare-earth elements doped in glass systems for radiation shielding where the results showed that the glass systems displayed significantly better shielding properties. A previous work highlighted the significance of erbium doped tellurite glasses where the mass attenuation coefficients (μ/ρ) and the effective atomic numbers (Z_{eff}) were determined for the glass systems at photon energies of 20 keV, 30 keV, 40 keV and 60 keV using WinXcom. The results showed that overall the erbium doped tellurite glasses showed significantly better shielding properties [37]. Another work also using WinXCom studied the mass attenuation coefficients (μ/ρ), effective atomic number (Z_{eff}) and the electron density (N_e) of strontium doped borate glasses and results showed that the (μ/ρ) and Z_{eff} values increased with the increase in the Bi_2O_3 content [38].

4. Conclusion

As expected, the addition of thulium oxide (Tm_2O_3) into the glass system as the dopant attenuates more gamma irradiation and improves the radiation shielding properties. The results show that the mass attenuation coefficient (μ_m) increases as the Tm_2O_3 concentration increases. Glass sample 3.0TmBiBT with composition of 3.0% mol of Tm_2O_3 gives the highest mass attenuation coefficient (μ_m) in the energy range of 1keV-100GeV. This indicates that the $(B_2O_3)_{0.170}(TeO_2)_{0.5}(Bi_2O_3)_{0.3}(Tm_2O_3)_{0.030}$ glass is more efficient in attenuating more gamma rays and in providing better shielding in the selected energy range. The results also show that all the shielding parameters, the mass attenuation coefficient (μ_m) the effective atomic number (Z_{eff}) and the electron density (N_e) in the energy range of 1 keV – 100 GeV, are very much affected by the incoming gamma photon energy and the glass chemical composition. The interactions between the photons and the glass materials are explained by the Photoelectric Effect, Compton Scattering and Pair Production. In conclusion, the theoretical results of this study demonstrates the advantages of the bismuth-boro-tellurite glass doped with thulium oxide as a new candidate for gamma radiation shielding material in the selected energy range.

Acknowledgements

The authors appreciate the financial support from the Universiti Pertahanan Nasional Malaysia, under GPJP, grant no. UPNM/2019/GPJP/2/SG/6.

References

- [1] G. Lakshminarayana, I. Kebaili, M. G. Ding, M. S. Al-Buriahi, A. Dahshan, I. V. Kityk et al., *J. Mater. Sci.* 55, 5750 (2020); <https://doi.org/10.1007/s10853-020-04446-4>
- [2] M. K. Halimah, A. Azuraida, M. Ishak, L. Hasnimulyati, *J. Non-Cryst. Solids* 512, 140 (2019); <https://doi.org/10.1016/j.jnoncrysol.2019.03.004>
- [3] M. S. Al-Buriahi, M. Rashad, A. Alalawi, M. I. Sayyed, *Ceram. Int.* 46, 16452 (2020); <https://doi.org/10.1016/j.ceramint.2020.03.208>
- [4] K. A. Naseer, K. Marimuthu, M. S. Al-Buriahi, A. Alalawi, H. O. Tekin, *Ceram. Int.* 47, 329 (2021); <https://doi.org/10.1016/j.ceramint.2020.08.138>
- [5] C. Devaraja, G. V. Jagadeesha Gowda, B. Eraiah, K. Keshavamurthy, *Ceram. Int.* 47, 7602 (2021); <https://doi.org/10.1016/j.ceramint.2020.11.099>
- [6] Y. Anantha Lakshmi, K. Swapna, K. S. R. Krishna Reddy, S. Mahamuda, M. Venkateswarulu, A. S. Rao, *Opt. Mater.* 109, 110328 (2020); <https://doi.org/10.1016/j.optmat.2020.110328>
- [7] G. Lakshminarayana, M. I. Sayyed, S. O. Baki, A. Lira, M. G. Dong, K. A. Bashar, *J. Electron. Mater.* 48, 930 (2018); <https://doi.org/10.1007/s11664-018-6810-8>
- [8] G. Sathiyapriya, K. Marimuthu, M. I. Sayyed, A. Askin, O. Agar, *J. Non-Cryst. Solids* 522, 119574 (2019); <https://doi.org/10.1016/j.jnoncrysol.2019.119574>
- [9] M. I. Sayyed, A. A. Ali, H. O. Tekin, Y. S. Rammah, *App. Phys* 125, 445 (2019); <https://doi.org/10.1007/s00339-019-2739-x>
- [10] I. I. Kindrat, B. V. Padlyak, S. Mahlik, B. Kuklinski, Y. O. Kulyk, *J. Opt. Mater.* 59, 20 (2016); <https://doi.org/10.1016/j.optmat.2016.03.053>
- [11] R. Kaur, S. Singh, O. P. Pandey, *J. Molecular Structure* 1060, 251 (2014); <https://doi.org/10.1016/j.molstruc.2013.12.036>
- [12] C. Bootjomchai, J. Laopaiboon, C. Yenchai, R. Laopaiboon, *Radiat. Phys. Chem.* 81, 785 (2012); <https://doi.org/10.1016/j.radphyschem.2012.01.049>
- [13] R. Bagheri, A. Khorrami Moghaddam, H. Yousefnia, *Nucl. Eng. Tech.* 49, 21 (2017); <https://doi.org/10.1016/j.net.2016.08.013>
- [14] P. Kaur, K. J. Singh, S. Thakur, *AIP Conf. Proc.* 1953, 090031 (2018).
- [15] H. A. Saudi, H. M. Goma, M. I. Sayyed, I. V. Kityk, *SN App. Sci.* 1, 218 (2019); <https://doi.org/10.1007/s42452-019-0197-x>
- [16] N. Kucuk, S. R. Manohara, S. M. Hanagodimath, L. Gerward, *Radiat. Phys. Chem.* 86, 10 (2013); <https://doi.org/10.1016/j.radphyschem.2013.01.021>
- [17] A. Un, F. Demir, *J. Appl. Radiat. Isot* 80, 73 (2013); <https://doi.org/10.1016/j.apradiso.2013.06.015>
- [18] V. P. Singh, M. E. Medhat, S. P. Shirmardi, *Radiat. Phys. Chem.* 106, 255 (2015); <https://doi.org/10.1016/j.radphyschem.2014.07.002>
- [19] D. K. Gaikwad, P. P. Pawara, T. P. Selvam, *Radiat. Phys. Chem.* 138, 75 (2017); <https://doi.org/10.1016/j.radphyschem.2017.03.040>
- [20] M. Esfandiari, S. P. Shirmardi, M. E. Medhat, *Radiat. Phys. Chem.* 99, 30 (2014); <https://doi.org/10.1016/j.radphyschem.2014.02.011>
- [21] S. D. Huse, S. S. Obaid, A. A. Joshi, D. K. Gaikwad, P. P. Pawar, A. R. Shitre, *J. Phys.: Conf. Ser.* 1644, 012061 (2020); <https://doi.org/10.1088/1742-6596/1644/1/012061>
- [22] L. Gerward, N. Guilbert, K. B. Jensen, H. Levring, *Radiat. Phys. Chem.* 71, 653 (2004); <https://doi.org/10.1016/j.radphyschem.2004.04.040>
- [23] P. Limkitjaroenporn, J. Kaewkhao, P. Limsuwan, W. Chewpraditkul, *J. Phys. Chem. Solids* 72, 245 (2011); <https://doi.org/10.1016/j.jpcs.2011.01.007>
- [24] J. Kaewkhao, J. Laopaiboon, W. Chewpraditkul, *J. Quant. Spectrosc. Radiat. Transf.* 109, 1260 (2008); <https://doi.org/10.1016/j.jqsrt.2007.10.007>
- [25] G. Lakshminarayana, M. I. Sayyed, S. O. Baki, A. Lira, M. G. Dong, K. M. Kaky et al, *Appl. Phys. A* 124, 378 (2018); <https://doi.org/10.1007/s00339-018-1801-4>

- [26] A. Azuraida, M. K. Halimah, A. A. Sidek, C. A. C. Azurahaman, S. M. Iskandar, M. Ishak, Chalcogenide Lett. 12, 497 (2015).
- [27] S. A. M. Issa, A. M. A. Mostafa, J. Alloys Compd. 695, 302 (2017); <https://doi.org/10.1016/j.jallcom.2016.10.207>
- [28] E. S. A. Waly, M. A. Fusco, M. A. Bourham, Ann. Nucl. Energy 96, 26 (2016); <https://doi.org/10.1016/j.anucene.2016.05.028>
- [29] M. E. Çelikkbilek, A. E. Ersundua, M. I. Sayyed, G. Lakshminarayana, S. Aydın, J. Alloys Compd. 714, 278 (2017); <https://doi.org/10.1016/j.jallcom.2017.04.223>
- [30] A. Saeed, Y. H. Elbasha, R. M. El Shazly, Opt. Quantum Electron 48, 1 (2016). <https://doi.org/10.1007/s11082-015-0274-3>
- [31] R. Polat, Z. Yalcın, O. İc-elli, Nucl. Instruments Methods Phys. Res. A 629, 185 (2011); <https://doi.org/10.1016/j.nima.2010.11.001>
- [32] N. Chanthima, J. Kaewkhao, Ann. Nucl. Energy 55, 23(2013); <https://doi.org/10.1016/j.anucene.2012.12.011>
- [33] M. Kurudirek, Y. Ozdemir, O. Simsek, R. Durak, J. Nucl. Mater. 407, 110 (2010); <https://doi.org/10.1016/j.jnucmat.2010.10.007>
- [34] C. İpbuker, H. Nulk, V. Gulik, A. Biland, A. H. Tkaczyk, Nucl. Eng. Des. 284, 27 (2015); <https://doi.org/10.1016/j.nucengdes.2014.12.007>
- [35] S. R. Manohara, S. M. Hanagodimath, Nucl. Instruments Methods Phys. Res. B 258, 321 (2007); <https://doi.org/10.1016/j.nimb.2007.02.101>
- [36] F. Akman, R. Durak, M. F. Turhan, M. R. Kacal, Appl. Radiat. Isot. 101, 107 (2015); <https://doi.org/10.1016/j.apradiso.2015.04.001>
- [37] S. A. Tijani, S. M. Kamal, Y. Al-Hadeethi, M. Arib, M. A. Hussein, S. Wageh, J. Alloys Compd. 741, 293 (2018); <https://doi.org/10.1016/j.jallcom.2018.01.109>
- [38] M. I. Sayyed, G. Lakshminarayana, M. G. Dong, M. E. Çelikkbilek, A. E. Ersundu, I. V. Kityk Radiat. Phys. Chem. 145, 26 (2018); <https://doi.org/10.1016/j.radphyschem.2017.12.010>